DOI: 10.1016/j.nima.2020.164874
Report number: FERMILAB-PUB-21-138-TD
(accepted)

Assessment of Operational Availability for the PIP-II Superconducting Radio Frequency Linear Accelerator Facility

A. Saini[†1], R. Prakash[††1,2,3], J. D. Kellenberger[1]

[1]Fermi National Accelerator Laboratory, Batavia IL 60510, USA,

[2]Raja Ramanna Centre for Advanced Technology, Indore 452013, India

[3]Homi Bhabha National Institute, Anushaktinagar, Mumbai 400094, India

Abstract

Operational availability is a critical performance measure for an accelerator facility in modern time. A high availability enables the facility to serve a wide range of users simultaneously. Consequently, besides pure accelerator physics considerations, newly proposed accelerator facilities account for the availability and reliability aspects in the design phases. It allows incorporation of appropriate mitigation strategies for the most vulnerable systems in the machine and therefore, minimizes unscheduled interruptions during the operation. This paper lays out a methodology for the availability assessment of the complete particle accelerator facility and presents an initial assessment of the availability of the newly proposed Proton Improvement Plan-II (PIP-II) accelerator facility at Fermilab. The paper describes a comprehensive reliability model of the PIP-II facility that comprises not only 800 MeV linear accelerator (linac) system but also essential utility systems in the form of cryogenic, water, power and air systems. The paper details estimations of the availability of the PIP-II facility for two operational modes i.e. the nominal operational mode featuring 800 MeV beam and critical operational mode involving operation with the lowest objective beam energy of 600 MeV.

Revised Date :16 November 2020

I. INTRODUCTION

Availability analyses have been a standard protocol in industries where the operational costs are taken into account at design level of a new product. However, practice of the reliability engineering in research infrastructures, that are usually driven by a fixed construction cost, is relatively new. The late introduction of the reliability engineering in the particle accelerator design is mainly due to a very complex nature of the machine. Every particle accelerator is unique in the

[†] asaini@fnal.gov, [††]rprakash@rrcat.gov.in,
Phone Number +6308405293,
Fermi National Accelerator Laboratory, Batavia IL, 60510

design and operation. Thus, input data required for such analyses are usually limited and specific to a given system. This adds uncertainty against realization of the reliability engineering aspect in the accelerator design. However, this trend has been changing lately and the modern accelerator facilities are anticipating importance of the reliability engineering in the accelerator design.

Most of newly proposed accelerator facilities around the world such as Linac Coherent Light Source-II (LCLS-II) [1], European Spallation Source (ESS) [2], Indian Spallation Neutron Source (ISNS) [3], China Accelerator Driven System (CADS) [4], etc. are based on the Superconducting Radio Frequency (SRF) technology. Recent advancements in the SRF technology make its usage more practical and cost effective for large accelerator facilities as well as for the commercial applications. The SRF technology brings in multiple advantages to an accelerator facility. It enables not only a high duty beam operation but also facilitates a high accelerating gradient in the cavities. With all numerous benefits, the SRF technology also brings in an adverse feature in terms of the additional complex systems (cryostat, cryo-plant, cryogen distribution etc.) needed for its implementation to an accelerator facility. Furthermore, repair or replacement of a malfunctioned superconducting component is both expensive and time consuming. Restoring a nominal accelerator operation after an interruption also takes time. This in turn, reduces overall availability of an accelerator. Consequently, modern SRF accelerator facilities are sighting importance of the availability and reliability analyses [5-8] to reduce operational cost of the unreliable accelerators. To assure a reliable operation with the minimal unscheduled interruptions, the reliability engineering aspects need to be considered from the design phases of the SRF accelerators. Performing the availability analysis at various stages of the design enables identification of critical components with a higher probability of failure as well as prediction of the unscheduled down time during operations. This in turn, may allow developing a mitigation strategy for critical components, appropriate allocation of redundancy and, resources for spare and replacement parts.

In the past, the availability analysis for the particle accelerators was often carried out either for certain sub-systems of the machine (e.g. cryo-plant, RF system etc.) or considering a simple form of the major beamline elements [9-13]. For this reason, the paper lays out a methodology for the availability assessment of the complete particle accelerator facility. It describes a comprehensive reliability model for the availability assessment of the Proton Improvement Plan-II (PIP-II) SRF accelerator facility [14] that includes not only the accelerator components but also essential utility systems in terms of the water, air, cryogenic and power systems. Furthermore, the model implements the accelerator components in their detail composition that implies an accelerator component is described with its essential auxiliary systems. For an instance, an accelerator cavity in the model is implemented with its power coupler, frequency tuner and RF power source. Thereafter, the paper discusses studies for the PIP-II facility that lead to finding of the most critical section determining the unavailability budget of the PIP-II facility. Lastly, the paper converses the input data sensitivity analysis assessing impact

of a spread in the reliability input data on the model prediction and, validation of the model methodology using a reference model of the existing operational accelerator facility.

The paper is organized in seven sections. Section-II provides an overview of the PIP-II SRF linear accelerator whereas Section-III introduces key definitions and concepts of the availability analysis for an accelerator system. Section-IV discusses preparation of the PIP-II accelerator facility model and describes components selection criteria, operational modes and the high-level functional block diagram of the facility. Section-V converses results of the availability analyses while Section-VI presents a sensitivity analysis and the model benchmarking with an operational accelerating facility. The paper concludes with a summary in Section-VII.

II. PIP-II SRF LINAC ACCELERATOR FACILITY

Fermilab is planning to perform a systematic upgrade to its existing accelerator complex to support a world leading neutrino program. A comprehensive roadmap named "Proton Improvement Plan (PIP)" has been established. The second stage of the Proton Improvement Plan comprises construction of a new superconducting linear accelerator (linac) capable of accelerating a 2 mA H^- ion beam up to 800 MeV in a continuous wave (CW) regime. However, the initial operational goal is to deliver a 1.1% duty factor pulsed beam to the existing Booster synchrotron [15]. The PIP-II accelerator facility aims at the operational availability of 90% over a fiscal year [16]. Table 1 summarizes the most relevant operational beam parameters of the PIP-II linac.

Table 1: Design specifications for operational beam parameters of the PIP-II linac.

Parameter	**Magnitude**	**Units**
Final beam energy	800	MeV
Beam pulse repetition rate	20	Hz
Beam pulse length	0.55	ms
Average CW beam current	2	mA
Final ε_z	<0.4	mm-mrad
Final ε_t	≤0.3	mm-mrad

ε_z normalized RMS longitudinal emittance; ε_t normalized RMS transverse emittance

A schematic of the SRF linac's architecture is shown in Figure 1. It is composed of a warm front-end and an SRF accelerating section. The warm front-end comprises an H^- ion source (IS) capable of delivering a 15 mA, 30 keV, DC or pulsed beam, a 2m long Low Energy Beam Transport (LEBT) line [17], a 162.5 MHz, CW Radio Frequency Quadrupole (RFQ) [18] that accelerates the beam to 2.1 MeV and a 13m long Medium Energy Beam Transport (MEBT) line [19] that

includes variety of diagnostic devices and a chopper system capable of generating an arbitrary bunch pattern before the beam is injected into the SRF section.

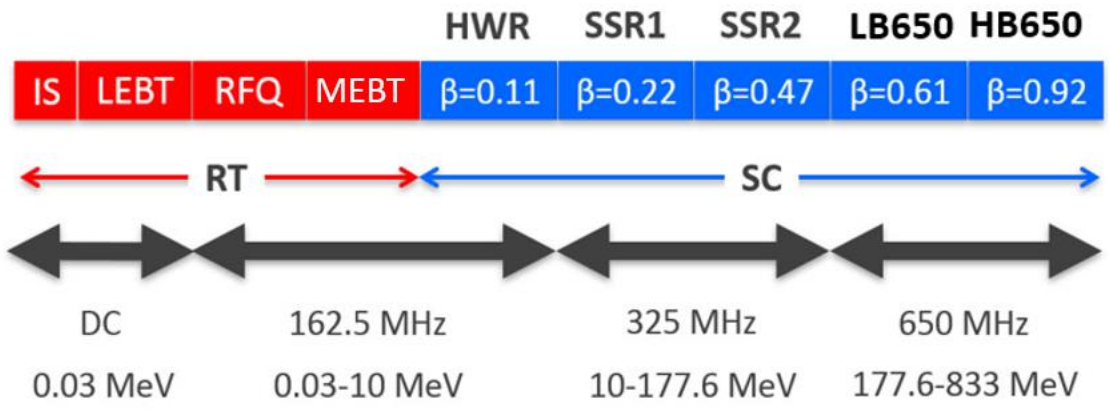

Figure 1: Block diagram representation of the PIP-II Linac. Red coloured blocks represent the warm sections whereas the blue blocks represent superconducting sections operating at 2K. Normalized design velocity (β) of the cavity in each section is also shown.

The MEBT is followed by the SRF linac that uses five families of SRF cavities to accelerate the beam up to 800 MeV. Based on these families, the linac is segmented into five SRF sections named as, Half Wave Resonator (HWR) [20], Single Spoke Resonator (SSR) 1 & 2 [21-22], and Low Beta (LB650) and High Beta (HB650) [23]. Table 2 highlights configuration of each section and includes details of a number of cryomodules (CM), focusing magnets and cavities as well as operating frequency of cavities and their accelerating ranges. Note that, superconducting solenoid magnets are used in the HWR, SSR1 and SSR2 sections whereas normal conducting (NC) quadrupole magnets arranged in doublet configuration are utilized in the LB650 and HB650 sections for the transverse beam focusing.

Table 2: Optics elements and transition energy in each section of the PIP-II SRF linac.

Section	**CM**	**Cav/Mag per CM**	**Operating Frequency**	**Energy (MeV)**
HWR	1	8/8	162.5 MHz	2.1-10
SSR1	2	8/4	325 MHz	10-32
SSR2	7	5/3	325 MHz	32-177
LB	9	4/1*	650 MHz	177-516
HB	4	6/1*	650 MHz	516-833

* Normal conducting quadrupole doublet

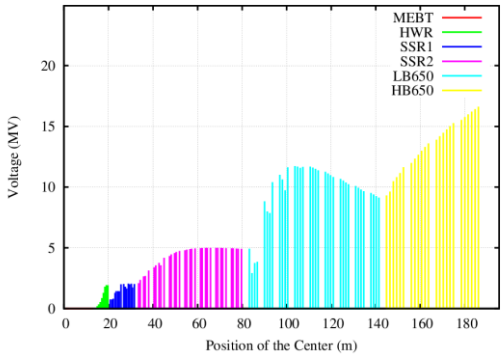

(a)

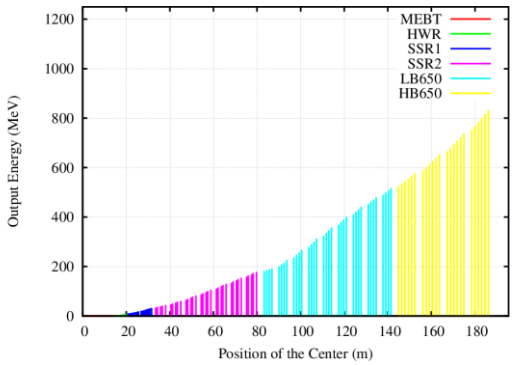

(b)

Figure 2: (a) Accelerating voltage and (b) output energy along the PIP-II linac for the nominal optics. Note that, the bunching cavities in MEBT operates at -90^0 synchronous phase and therefore provides no acceleration.

The linac optics has been carefully designed to deliver a high-quality beam at the Booster entrance. Figure 2 shows the accelerating voltage and output energy at each cavity along the linac for the baselined optics. Detailed description of the linac architecture and its optics design has been presented elsewhere [24].

III. AVAILABILITY FORMALISM FOR ACCELERATORS

There are many good text books [25-26] dedicated to the reliability engineering theory. For the comprehension of this article, this section introduces necessary theory and, discusses how it is applicable in the framework of accelerators.

The failure rate (λ) of a component through its life span usually follows a bath-tub distribution as shown in Figure 3. Initial portion of the bath-tub curve is called the burn-in period that consists of a high failure rate due to the infant mortality. Similar behaviour is observed at the end of the curve due to deterioration of components. This period is defined as

the wearing-out period. Between these two regions, a system has a useful life period which consists of a relatively lower and constant failure rate. Assuming, accelerators also follow the bath-curve analogy. The burn-in period is then referred to the commissioning period when the accelerators are being actively tuned and tested to deliver operational parameters. A wear-out period for the accelerators is the period when an upgrade or replacement is needed to maintain its operational performance. In this paper, the main emphasis is on the useful period of an accelerator which can be interpreted as its nominal operational period. In subsequent sections, the availability model is solved using the assumption of a constant failure rate of components. Note that, the assumption not only justifies the bath-tub analogy but also permits solving the model analytically which otherwise becomes too cumbersome to solve analytically for the large systems.

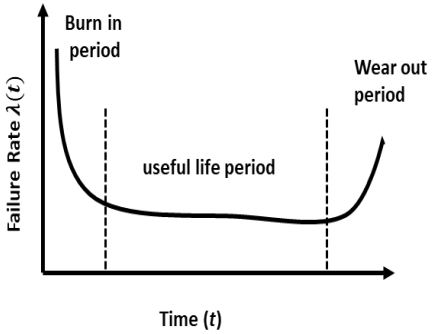

Figure 3: Evolution of the characteristic failure rate function of a system over a length of time.

The cumulative experience with existing operating accelerator facilities suggests a gradual degradation in performance of the accelerator components over a period of time. For instance, surface contaminations of the SRF cavities may reduce the maximum available accelerating gradient. These gradual degradations in the operational performance over time are called parametric drift failures in the reliability engineering. Adding a safety margin in the operational parameters and using new advances in the accelerator technology, such as plasma processing of the SRF cavities [27], and allowing others to address the parametric failures in the accelerators at some extent. Thus, in this article, it is assumed that a component has only two states of operation either a nominal working state or a failed state.

A. General Formalism

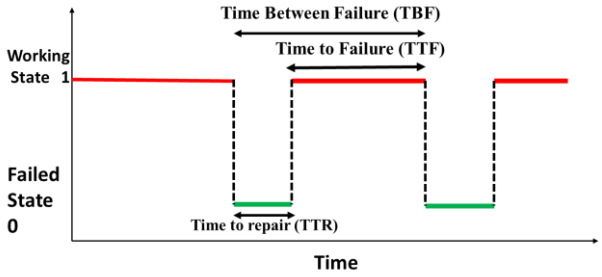

Figure 4: Evolution of operating states of a binary system with time.

Figure 4 illustrates a system which has only two operating states i.e. working state and failed state. The length of time for which the system keeps a working state is called Time to Failure (TTF) whereas the time taken to repair the system after a failure is termed as Time to Repair (TTR). The time between successive failed states is quantified as Time Between Failure (TBF). These times are collectively called the characteristic times of a system. In a n-component system there are several ways a system might fail and be repaired. Thus, it is more appropriate to determine the characteristics times from mean of respective distributions.

The Mean Time Between Failure (MTBF) is then expressed as:

$$MTBF = MTTF + MTTR; \quad (1)$$

where Mean Time To Fail (MTTF) is the statistical average of operating time and Mean Time To Repair (MTTR) is the statistical average of the repair time for a system. In case of a constant failure rate (λ), MTTF for a non-repairable system can be written as:

$$MTTF = \frac{1}{\lambda}. \quad (2)$$

The reliability of an accelerator is defined as the probability that it does not fail in a given mission time whereas the availability (A) is proportion of its "up time" to the total operational time over a defined operation period. It can be quantified as:

$$A = \frac{MTTF}{MTTF+MTTR}. \quad (3)$$

One can conclude from their definitions that the mean time between the failure and the failure rate are measures of the reliability. To obtain a high reliability and availability, an accelerator must avoid repetitive failures and long down time after a failure occurrence. Thus, decreasing the mean time to repair is one of the main design considerations. Common strategies to minimize MTTR include frequent monitoring of accelerator-systems to identify probable issues before failure occurrence; proper distribution of diagnostic devices to minimize diagnostic time, appropriate allocation of spares to

reduce logistics and minimizing the replacement time; establishing a dedicated team of experts to perform quick repairs, etc. It is clear that improvement in MTTR is achieved at the expense of an increase in overall cost of the facility. A balance must be obtained between objective MTTR and the resulting cost.

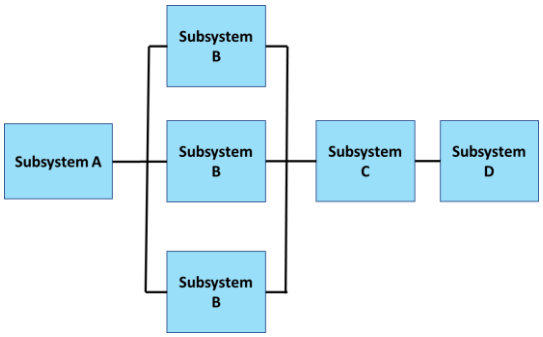

Figure 5: A reliability block diagram representing common system-component functional relationship in a complex system.

The foremost step in estimation of the availability of an accelerator is to obtain availabilities of individual components using their MTTF and MTTR input data. Then, the next step involves acquiring information of the component functional roles in the accelerator-system. This system-component functional relationship is often expressed in the form of a Reliability Block Diagram (RBD) where each component is represented in the form of a block. Figure 5 shows the most common system-component functional relationship. In this example, the components are connected in a series (failure of a component leads to a failure of the overall system, similar to the logical AND gate analogy) and in parallel arrangements (failure of a component will not lead to a failure of the overall system until all parallel connected components get failed, similar to the logical OR gate analogy). Note that series and parallel connections are a limiting case of the "k out of n" system where the availability of a system with *n* identical components is obtained as following:

$$A(t)_{sys\,(r\leq k)} = \sum_{r=0}^{k} \frac{n!}{r!(n-r)!} A(t)^{n-r}(1-A(t))^{r} \qquad (4)$$

where r is number of failures, *k* is maximum allowable failures and *A(t)* is the availability of the component at time *t*. When *k=0*, all components are connected in series while for $k = n - 1$, all components are connected in parallel.

In an accelerator, a variety of component-system functional relationships such as series, parallel, standby, redundant connects etc., might exist simultaneously. A list of formulae for the system availability and reliability with such configurations has been presented in the Appendix-A1.

IV. AVAILABILITY ASSESSMENT MODEL FOR PIP-II

A comprehensive availability assessment model of the PIP-II accelerator facility in form of the high-level functional block diagram is developed to compute its availability. This section details preparation of the model and delineates assumptions and guidelines used to build the model.

A. Component Selection

It is evident that an accelerator comprises numerous components and dependent systems. Many of these components need additional auxiliary elements to execute their nominal function. For instance, an accelerating cavity assembly in the beamline is comprised of several auxiliary elements such as, power coupler to feed RF power; a mechanical tuner to tune its resonant frequency etc. This in turn, adds another layer of elements in the model. Consequently, the model of an accelerator facility becomes very large and cumbersome. In order to resolve this issue, a component-selection criterion was applied to the PIP-II model. A component features any of following characteristics is included in its detailed composition as practically permissible while preparing the model of the PIP-II facility.

- Components having moving parts such as vacuum pumps, cavity tuners etc.
- Components operating in pulsed mode such as high voltage switches, kicker system in the MEBT etc.
- Components that are involved in thermal cycling processes *e.g.* heat exchangers for low conductivity water (LCW).
- Components containing a high stored energy, *e.g.* RF cavities and magnets etc.
- Components involved in the high current operations *e.g.* modulators.
- A larger set of commercial components as they might not be designed for high reliability.

Note that, components exhibiting above characteristics are relatively more vulnerable to failures and therefore, drive the overall availability of the PIP-II facility.

B. Model Assumptions

The model uses the following assumptions to compute the availability of the PIP-II facility:

- As also mentioned earlier, each component in the model possesses only binary states of the operation i.e. either operating nominally or failed. The component can migrate any state independent of its history of the operation.
- A component exhibits a constant failure rate during its operation.
- Each component fails at a random time with an exponential distribution determined by its MTBF. Two simultaneous failures are prohibited in the model. Those uncorrelated component failures are then represented by the Markov chains [26] and solved analytically to evaluate the system availability.

- When a component fails, it leads to the system failure (unless fault-tolerances are specified) resulting in an unscheduled accelerator shut-down. A temporary component failure such as one resulting from quenching of an SRF cavity or magnet is not treated as a failure in the model.
- The model assumes components meet their design specifications and the system is maintained to its best operable condition. Thus, the model does not incorporate manufacturing errors, human errors and environmental errors. Additionally, implications of the drift failures or degradation in performance of components are not included in the model.
- The model implements only corrective maintenance. It implies the fault detection time, logistic time at various stages of repair, tuning etc. are excluded. As soon as a failure is detected, the maintenance process is launched. After a repair, the component is treated "as good as new". Thus, resulting availability of the system is called inherent availability. Note that, the availability in this paper is always attributed to the inherent availability.
- The model is further simplified with the assumption that the facility transits from a no-beam state after a failure to the nominal beam state as soon as a repair is completed.
- A mission time of about a year, equivalent to eight thousand operational hours, is assumed for the availability analysis of the PIP-II accelerator facility.

C. Operational Modes

A system can require to operate in different modes. These operational modes define the system-component functional relationship and therefore, a failure pattern of the system. Consequently, the system operational availability may vary from one operational mode to another. Thus, it is essential to establish operational modes of a system before estimating its availability. In this article, the availability of the PIP-II accelerator facility is evaluated for two operational modes named as the nominal operational mode and critical operational mode.

1. Nominal Operational Mode

In the nominal operational mode, the PIP-II facility delivers 800 MeV beam to the Booster synchrotron with the design specifications listed in Table 1. Note that, the baseline configuration of the SRF linac has been designed to accelerate the beam up to 833 MeV. This additional energy provides a safety margin to achieve the nominal operational mode. It has been shown elsewhere [28-29] that the SRF linac optical design is sufficiently robust to tolerate a failure of optical element in each SRF section without conceding the design specifications. Consequently, the nominal operational mode can be achieved in two ways. The first nominal operational scenario, termed as no-failure-permit in this paper, involves all optical elements are operating with their design parameters. In this configuration, any component failure will produce a complete

system failure. The second scenario is named as the fail-tolerance operation that permits a faulty/malfunctioned accelerating cavity in each SRF section (HWR, SSR1, SSR2, LB650 and HB650). It implies that the facility would keep operating even after a failure of the SRF cavity in each section. Note that, a repair or replacement of an element in cryogenic environment requires relatively a longer time in comparison to repair of a normal-conducting element. Consequently, the fault-tolerances in the availability estimate have been included only in SRF sections. This choice for the analysis does not infer the fault-tolerance capability of the normal-conducting sections and, allows a conservative estimate of the availability. It is worth to mention that a conservative assessment is beneficial at the design phase where a number of factors (human errors and environmental impacts) are relatively less known.

2. Critical Operational Mode

The lowest permissible beam energy out of the linac, at which the PIP-II facility could sustain an operation, is specified to be 600 MeV. This energy is called the critical threshold energy below which Booster synchrotron operation becomes incompatible due to excessive beam losses. Availability assessment of the PIP-II facility is also performed for this mode where the linac delivers 600 MeV beam with same rest of specifications as listed in Table 1.

V. AVAILABILTY ASSESSMENT FOR PIP-II FACILITY

A. Input Data

The reliability input data, MTTF and MTTR, for components are acquired from various sources including educated guess from the subject experts, operational experience with similar components at Fermilab as well as existing accelerator facilities, and from prototype tests. The beam commissioning of the PIP-II front-end at the Proton Improvement Plan-II Injector Test (PIP2IT) facility [30] also provided a useful information about operational reliability of the PIP-II components such as ion-source, magnet power supplies etc. A few components were commercially available and therefore, corresponding data were readily available. In addition, a few references [5-13] were also used to obtain data that were unavailable otherwise.

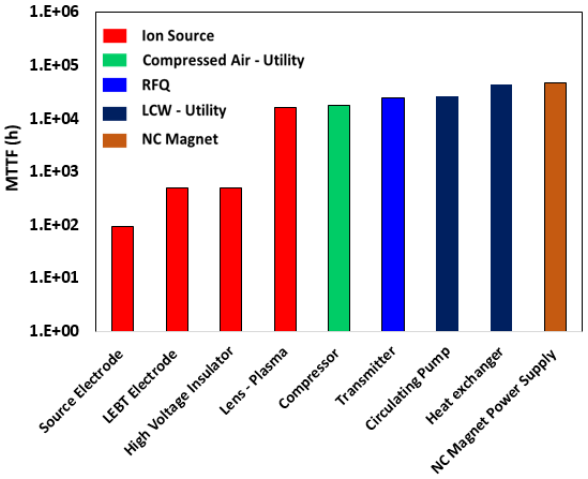

Figure 6: Components with the minimum MTTFs in the PIP-II model. The colour of the bar represents the component's association with respective assembly or section. For instance, red coloured bar shows the MTTF of components in the ion-source assembly.

Figure 6 shows most vulnerable components in the PIP-II accelerator facility model. It can be noticed from the Figure 6 that components in the ion source assembly possess the minimum MTTF that are followed by the compressor in the air utility system. Figure 7 shows the most robust and reliable components of the PIP-II facility model that have longest MTTF. Note that, a high MTTF implies less frequent failures of the component.

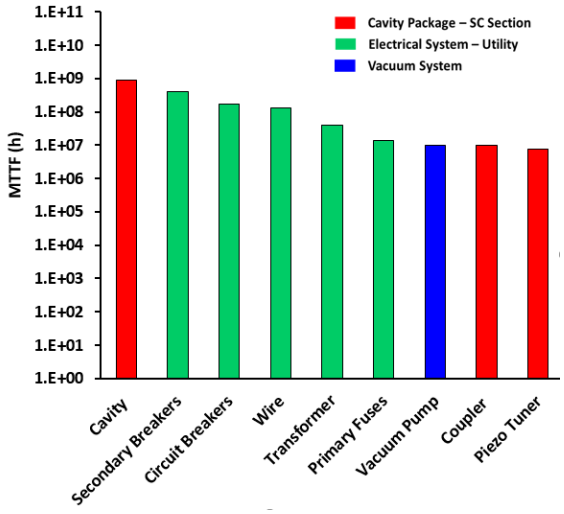

Figure 7: Components with the maximum MTTF in the PIP-II facility model. The colour of the bar represents the component's association with respective assembly or section. For instance, red coloured bars represent components in a superconducting (SC) cavity assembly.

It can be noticed from Figure 8 that the high voltage transformer in the electrical power grid and the SRF cavities acquire longest MTTR in the model. Based on previous experience at Fermilab, experts suggest that a repair/replacement of such transformer could take up to full two weeks. Considering an eight-hours work shift per day, the repair time is then

estimated to more than 1000 hours (24x3x14 >1000 h). Because of this, the PIP-II facility envisions two power lines. Electric-power loads is swiftly shifted from one line to another in case of a failure. A repair is then performed in parallel without a long interruption. Also note that, repair of an SRF cavity may need warming of the cryomodule from a cryogenic temperature to the room temperature, taking cryomodule out from the accelerator tunnel and then, dismantle it to replace/repair the faulty cavity. It could result in a long unscheduled down time spanning over several months. To minimize this time at the PIP-II facility, the mitigation strategy involves replacing the faulty cryomodule with a fully-functional spare cryomodule. Then, repair of the faulty-element in the cryomodule is carried out in parallel without affecting the accelerator operational time. This strategy restricts the repair time of a superconducting element to only about a month.

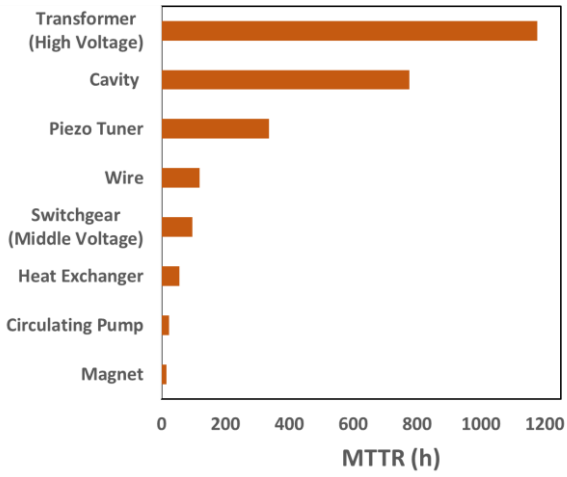

Figure 8: Components with the longest MTTR in the PIP-II facility model.

B. High-Level functional diagram for the PIP-II Facility

As a next step for the availability assessment, a high-level functional block diagram model of the PIP-II facility was developed. The facility, as shown in Figure 9, was modelled in two main parts: Utility systems and linac systems.

1. Utilities systems

A utility system in the model indicates a central facility of the core supply essential to operate an accelerator such as a cryo-plant to supply the cryogen for the SRF cavities. The model incorporates four utility systems that are subsequently discussed in detail.

- *Electrical-Power System:* The PIP-II accelerator facility envisions two electrical-power substations where one of the substations is available in the standby mode. In an event of failure, the power-load is swiftly shifted to the standby substation. The model includes major electrical components such as transformers, switchgears, fuses, circuit breakers and cables. The most vulnerable component in the electrical system is the Vacuum Circuit Breaker (VCB) which exhibits a

higher failure rate. Because of this, four out of every eight VCBs are redundant in the electrical system. Note that, the model does not incorporate the power generating system but only the supply system.

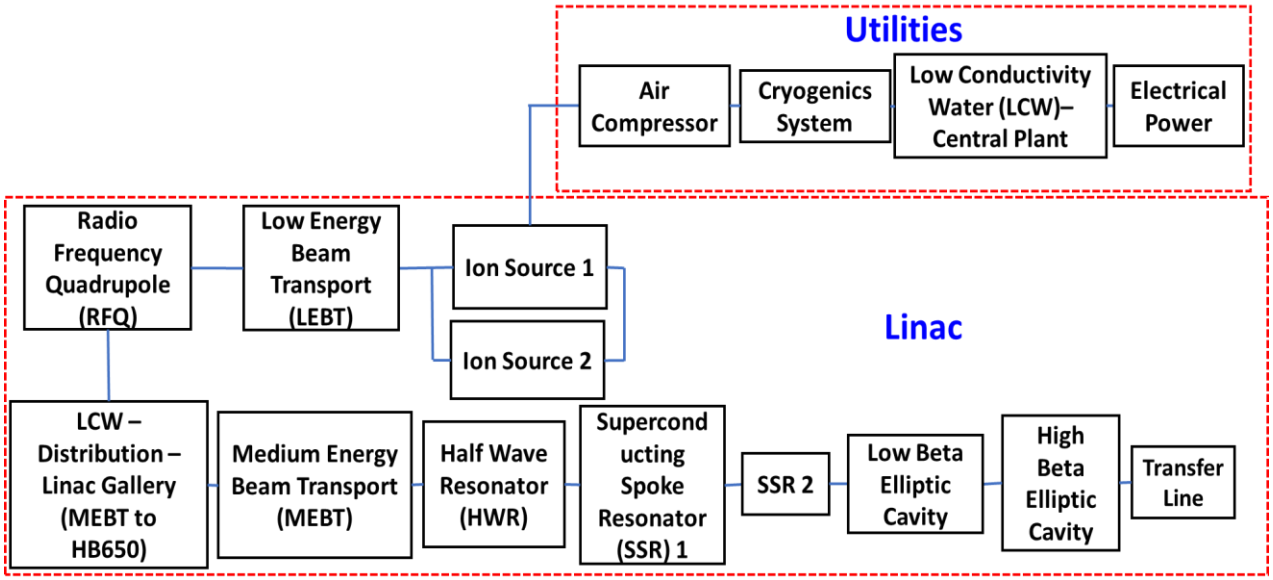

Figure 9: High level functional diagram for the PIP-II accelerator facility.

- *Cryo-plant System:* A cryo-plant supplies the cryogen necessary to maintain cryogenic temperature of the superconducting cavities. The main components of the cryo-plant included in the model are the cold compressors, turbines, expanders, warm compressors and, associated control systems. The warm compressors are the most susceptible to failures among the cryo-plant components.
- *Low Conductivity Water (LCW) System:* It delivers water to maintain the operating temperature of normal conducting water-cooled elements such as the RFQ. The LCW system includes circulating pumps, heat exchangers, gauges, transducers, flow meters and, valves. Among those components, the circulating pumps are more often involved in the failures. Consequently, the LCW system of the PIP-II facility includes a redundant unit per three circulating pumps.
- *Compressed Air System:* The air system supplies compressed air for cooling of the radiation-cooled components, actuation and control of pneumatic valves etc. Two main components of the air-system are the compressor, and dryer. Each of them has a redundant unit in the model.

2. Linac System

The model includes a detailed description of the accelerator system. Along with the SRF linac (described in Section-II), details of the the Beam Transfer Line (BTL) [31] were also included in the model. The BTL line is used to transport the beam from the end of the SRF linac to the Booster entrance. It is about 350m long and mainly composed of normal conducting quadrupole and dipole magnets.

As shown in Figure 9, the utility systems are connected to the linac in a series configuration. It implies failure of any functional blocks will shut-down the complete facility. After establishing the component-system functional relationship, the PIP-II accelerator facility model was incorporated in a Python-based program. The program has been developed at Fermilab to automate the availability assessment. It not only computes availability of the complete facility but also for the individual section and component. This feature facilitates finding the most vulnerable section determining overall availability of the facility.

C. Case Study of Availability Assessment for HWR Section

In order to illustrate how the availability assessment is performed, this section discusses a detailed case study for the HWR section and describes the methodology applied to evaluate the availability of the complete PIP-II facility.

The HWR section is the first SRF section in the PIP-II linac. As shown in Table 2, it consists of one cryomodule that comprises eight solenoid magnets and same number of HWR cavities. Each solenoid magnet includes the steering magnets to correct the beam trajectories in horizontal and vertical planes. Those beamline elements further need auxiliary components to execute their nominal operation. Thus, it is more appropriate to describe an essential element in terms of the package including all supporting components. The cryomodule model is then represented using six packages: cavity, RF control, magnet assembly, steerer assembly, vacuum system and local cryogenic system packages. Table 3 lists major components and their functions in respective packages for the HWR cryomodule.

Table 3: Components and their functions in the respective packages in the HWR cryomodule.

Component	Function
Cavity Package	
Cavity	Acceleration, longitudinal beam focussing
Tuner	Tune cavity resonant frequency
Power coupler	Feeding RF power to cavity
Interlock sensors and electronics	Sensors and electronics
Low Level RF	RF control and instrumentation
Solid state Amplifier (SSA)	RF power source
RF Control Package: SSA Control and Timing	
SSA controls	RF controls to SSA
SSA timing	Timing to the SSA
Magnet Assembly Package: Solenoid Magnets Assembly	
Magnet Power Supply	Power supply to solenoids
Magnet	Transverse focusing of the beam.
Magnet Instrumentation	Control system
Steering Assembly Package	
Steering Magnet	Beam Trajectory Correction
Steering Power Supply	Magnet power supply
Vacuum System Package	
Vacuum Valves	Maintain vacuum
Vacuum. Pump	Creating vacuum in the beam-line
Vacuum pump power supply	Powering the vacuum pump
Local Cryogenic System Package	
Local cryogenic system	Cryogenic distribution, cryostat structure and control

Availability assessment for the HWR cryomodule is performed for two operational modes: no-failure-permit and a cavity-fail-tolerance. In a no-failure-permit mode, failure of any component leads to failure of the complete HWR cryomodule whereas in, a cavity-fail-tolerance mode, the cryomodule keeps operating even after failure of one out of any eight SRF cavities. Figure 10 illustrates the functional block diagrams of the HWR cryomodule describing logical connections among element packages for two operational modes. In the no-failure-permit mode, all elements packages are connected in the series configuration (figure 10(a)). In a cavity-fail-tolerance mode (figure 10(b)), all element packages are connected in series with the cavity packages that are configured in seven out of eight arrangement.

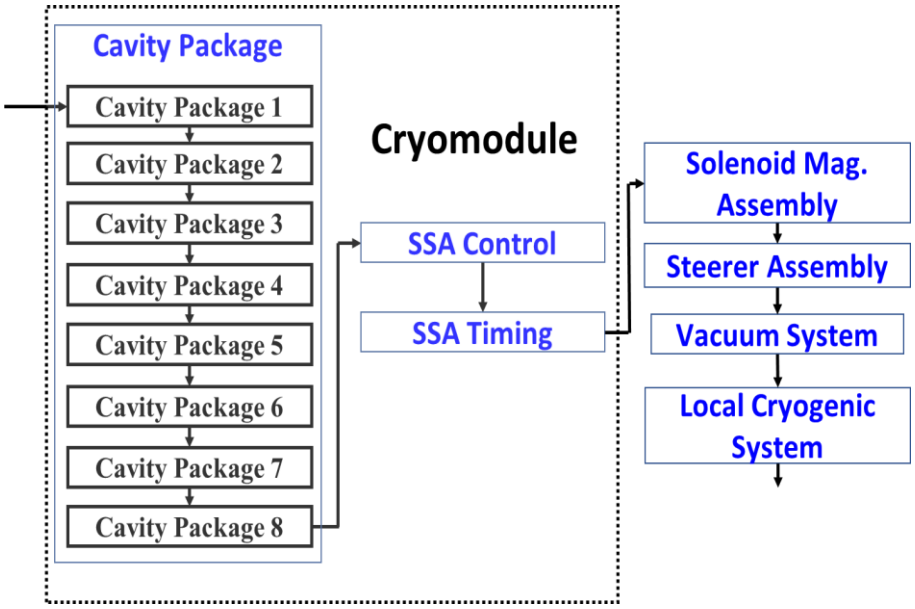

(a)

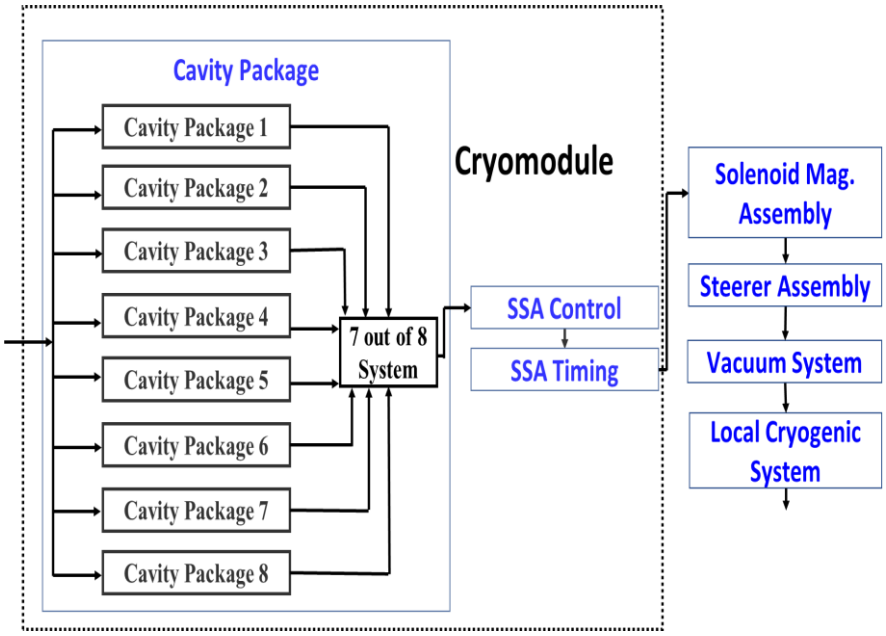

(b)

Figure 10: Functional block diagram for the HWR cryomodule for two operational modes :(a) no-failure-permit and (b) a cavity-fail-tolerance.

After establishing the functional diagram for the HWR cryomodule, next step involves computing availability of individual component in an element package using input data of MTTF and MTTR in equation (3). Table 4 shows availabilities of components in the cavity and magnet packages. Then, using the knowledge of components logical connections in an element package, availability of the package is evaluated. Since components are connected in series configuration in the packages, availability of a package is obtained using equation:

$$A_p = \prod_{i=1}^{N} A_i \qquad (5)$$

where A_p is the element package availability, A_i is the availability of i^{th} component in the package and N is total number of components in a package. Similarly, failure rate of the$\lambda_p = \sum_{i=1}^{N} \lambda_i$ element package is computed as:

$$\lambda_p = \sum_{i=1}^{N} \lambda_i \qquad (6)$$

where λ_p is the failure rate of an element package and, λ_i is the failure rate of individual components connected in a series configuration. As shown in Table 4, the failure rate of the cavity and magnet packages are 3.45E-05 and 1.2E-05 per hour respectively. Thereafter, the combined availability (A_{cp}) and Mean Time Between Failure $MTBF_{CP}$ of the packages are obtained after accounting for total number of the respective package and logical arrangement among them in the HWR cryomodule. It can be noticed from Table 4 that the combined availability of the cavity package in the HWR cryomodule was computed to be 99.79 % for the no-failure-permit mode and 99.99 % for a cavity-fail-tolerance mode. The combined availability of the solenoid magnet assembly package was obtained to be 99.989%. Similarly, combined availabilities of the rest of the packages in the HWR cryomodule were computed. Figure 11(a) shows the combined availability of all element package in the HWR cryomodule. Note that, without a fail tolerance, the cavity package offers the least combined availability. Since all element packages are connected in a series configuration with the cavity package (as shown in Figure 10), availability of the full HWR cryomodule is simply obtained from the product of their combined availabilities as depicted in Figure 11 (b). Resulting availability of the HWR cryomodule was obtained to be 99.69 % for the no-failure-permit mode that increases to 99.90 % for a cavity-fail-tolerance mode.

To benchmark this calculation, availability assessment of the HWR cryomodule for the no-failure-permit mode was performed using a trial version of commercially available Monte-Carlo simulation package BlockSim [32]. The results were in good agreements with our estimation as shown in Appendix-2.

403 Table 4: Availability of the cavity package and the solenoid magnet assembly package in the HWR cryomodule.

Component	MTTF (T) (h)	$\lambda\ (h^{-1})$	MTTR (h)	A_i (%)	$MTBF_{cp}$ (h)	A_{cp} (%)
Cavity Package						
Cavity	8.76E+08	1.14E-09	776	99.999	**Case 1: No-Failure-Permit mode**	
Tuner	1.00E+06	1.00E-06	216	99.978	8 cavity packages in series $MTBF_{CP} = \frac{1}{8\lambda_p}$ = 3623.19	8 cavity packages in series $A_{CP} = (\mathrm{A_p})^8$ A_{CP} = 99.79
Coupler	1.00E+07	1.00E-07	0.5*	99.999		
Interlock Sensors	1.00E+05	1.00E-05	1	99.999		
Interlock Electronics	1.00E+05	1.00E-05	1	99.999	**Case 2: A Cavity-Fail-Tolerance**	
Solid state Amplifier (SSA)	2.98E+05	3.36E-06	6	99.997	7 out of 8 cavity packages $MTBF_{CP} = \frac{1}{\lambda_p}\left(\frac{1}{8}+\frac{1}{7}\right)$ $MTBF_{CP} =$ 763.98	7 out of 8 cavity packages $A_{CP} = A_{CP} = (\mathrm{A_p})^8 + 7 \times (\mathrm{A_p})^7 \times (1 - \mathrm{A_p})$ A_{CP} =99.999
SSA Low Level RF	1.00E+05	1.00E-05	1	99.999		
		$\lambda_p = \sum_i^7 \lambda_i$ λ_p =3.45E-5		$A_{p=}\prod_{i=1}^{7} A_i$ $A_{p=}$99.97		
Solenoid Magnet Assembly						
Magnet Power Supply	1.00E+06	1.00E-06	2	99.992	8 Solenoid magnet assemblies are in series $MTBF_{CP} = \frac{1}{8\lambda_p}$ = 10416.67	8 Solenoid magnet assemblies are in series $A_{cp} = (\mathrm{A_p})^8$ A_{cp} =0.999
Magnet	1.00E+06	1.00E-06	792	99.999		
Magnet controls	1.00E+05	1.00E-05	2	99.998		
		$\lambda_p = \sum_i^3 \lambda_i$ λ_p =1.2E-5		$\mathrm{A_p} = \prod_{i=1}^{3} A_i$ $\mathrm{A_p} = 99.989$		

404 * It is assumed that the coupler MTTR is the time needed to restore accelerator operation after detuning the cavity. Major
405 coupler repairs are accounted in the cavity MTTR.
406
407
408
409
410
411
412

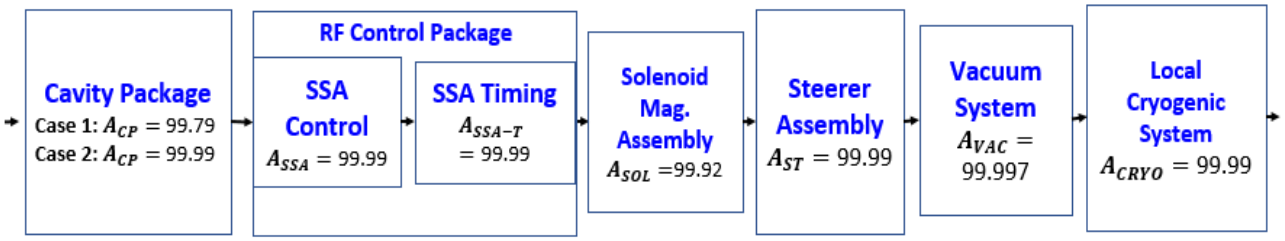

(a)

$$A_{HWR} = A_{CP} \times A_{SSA} \times A_{SSA-T} \times A_{SOL} \times A_{ST} \times A_{VAC} \times A_{CRYO}$$

No Failure Permit -Case 1 : 99.69
Cavity Failure Tolerance -Case 2 : 99.90

(b)

Figure 11: HWR cryomodule is modelled using six essential element packages that are connected in a series configuration with the cavity package. (a) Combined availability of each essential package and (b) availability of the full HWR cryomodule for two operational modes i.e. no-failure-permit (Case 1) and a cavity-fail-tolerance (Case 2).

D. Availability Assessment of the PIP-II Facility for Nominal Operational Mode

Availability of the full PIP-II facility for the nominal operational mode was modelled using the same methodology applied to the HWR section. Note that, as discussed earlier in Section-IV.C.1, there are two variants of the nominal operational mode i.e. no-failure-permit and fail-tolerance mode. In subsequent availability assessment, the fail-tolerance mode includes failure of an accelerating cavity in every SRF section.

The availability results show that an ion source offers the least availability of 89.08%. It is mainly because of the fact that the ion source requires the filament replacement for every three hundred hours of operation. Consequently, it creates a bottleneck on availability of the complete facility. To improve the ion source availability and therefore, for the complete facility, an additional ion source is installed in the standby configuration. In this arrangement, an ion source is always available for operation while others get repaired. This in turn, improves the ion source availability to 98.67 %. Table 5 lists availability of each sectional block (shown in Figure 9) of the PIP-II facility model for both nominal operational modes. In addition, it highlights the least available components/system-units in the respective sections. It is apparent from Table 5 that the transfer line possesses the least availability among all sections. Note that, the transfer line is about two

times longer than the SRF linac and, mainly composed of conventional normal conducting quadrupole and dipole magnets. The power supplies of the magnets exhibit a relatively higher failure rate with MTTF of ~4E+04 hours that brings down the availability of the section.

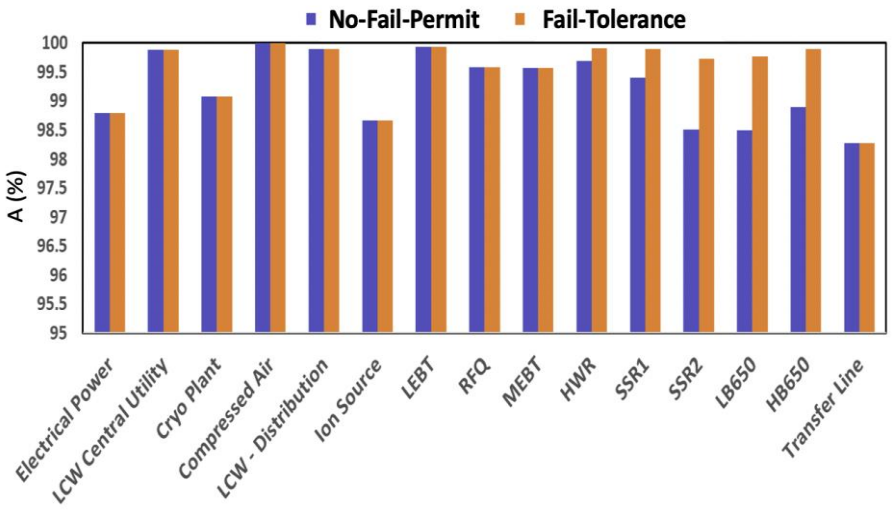

Figure 12: Availability of each section of the PIP-II facility for two variants of the nominal operational modes i.e. no-failure-permit mode (blue) and fail-tolerance mode (orange). Note that the fail-tolerance was applied only to the SRF section.

Figure 12 shows a comparison of availabilities obtained from two nominal operating modes. It is evident from Figure 12 that availabilities of the SRF sections substantially improve in the fail-tolerance mode.

Table 5: Availability of the functional blocks of the PIP-II facility for two nominal modes. The component with the least availability in respective section is also listed.

		Availability (%)		**Component with lowest availability in the section.**	
	Section	**No-Failure-Permit mode**	**Fail-Tolerance mode**	**Component Name**	**Availability (%)**
1	Electrical Power System	98.79	98.79	Electric Wire	99.22
2	LCW Central System	99.88	99.88	Pressure gauge	99.91
3	Cryo-plant System	99.07	99.07	Warm Compressors	99.82
4	Compressed Air System	99.99	99.99	Compressor	99.99
5	Ion Source	98.67	98.67	Individual Ion Source	89.08
6	LEBT	99.93	99.93	High Voltage Switch	99.95
7	RFQ	99.58	99.58	LCW- Distribution (RFQ)	99.70
8	LCW–Distribution	99.89	99.89	Circulating Pump	99.91
9	MEBT	99.57	99.57	Magnet Power Supply Chain	99.80
10	HWR	99.69	99.90	Solenoid Magnet	99.91
11	SSR 1	99.40	99.90	Solenoid Magnet	99.91
12	SSR 2	98.50	99.72	Solenoid Magnet	99.78
13	LB 650	98.49	99.76	Quadrupole Magnet Package	99.85
14	HB 650	98.89	99.89	Quadrupole Magnet Package	99.87

15	Transfer Line	98.27	98.27	LCW Distribution (Transfer Line)	99.09

To make it more suggestive for practical purposes, the PIP-II sectional blocks are grouped into three major systems i.e. Utility, NC and SRF linac. Table 6 lists the availability and MTBF of each major system. The SRF linac exhibits the lowest availability of 95 % for the no-failure-permit mode that increases to 99% after applying a cavity fail tolerance in every SRF section. Then, availability of the full PIP-II facility, computed from a product of the availability of every section, was found to be 89.2 % and 93.0 % for the no-failure-permit and fail-tolerance modes respectively. Again, all sections were connected in a series configuration in the PIP-II model (Figure 9). It should also be noted that the facility exhibits a higher MTBF of 74.5 hours in the fail-tolerance mode in comparison to 62.5 hours of the no-failure-permit mode. The MTTR of the PIP-II facility was computed using following equation:

$$MTTR = MTBF - A * MTBF \quad (7)$$

It results in the MTTR of 6.8 and 5.2 hours for the no-failure and fail-tolerance modes respectively.

Table 6: Availability and MTBF allocation by category for two operational modes of the PIP-II linac facility.

	No-Failure-Permit Mode		Fail-Tolerance-Mode	
	MTBF (h)	A (%)	MTBF (h)	A (%)
Utility system	1881.2	97.6	1881.2	97.6
NC Linac system	127.8	96.1	127.8	96.1
SRF Linac system	130.9	95.1	197.8	99.2
PIP-II Facility	62.5	89.2	74.5	93

The operational statistics of the existing accelerator facility corroborates that the target availability of 90 % is well within reach of the modern technology. The Spallation Neutron Source (SNS) accelerator facility at Oak Ridge [33] has been reporting an availability of 90% since 2011 [34-35]. The proposed ESS facility also targets the facility availability of at least 90% over a calendar year [7]. This in turn, confirms feasibility of the PIP-II availability target. It is apparent from Table 6 that the PIP-II accelerator facility can deliver the target availability of 90% over a fiscal year in both operational modes. However, the analysis also corroborates that an additional improvement in the availability can be achieved through gaining a capability of operation in a fail-tolerance mode. This is why the baseline design of the PIP-II linac [36] has adopted a cavity fault-tolerance in every SRF section. In addition to a local energy correction, allocation of a spare cavities per section enables optics tuning in case of malfunctioned elements which is otherwise not possible if spare cavities are located at the end of linac.

At times it is more practical to describe the unavailability in term of the down-time that can be estimated using following equation:

$$Down\ Time\ = (1 - A)T_{operation} \quad (8)$$

where, $T_{operation}$ is the total operational mission time. Based on the operational mission time of *8000* hours (excluding scheduled maintenance), the down-time of each section of the PIP-II facility was estimated. As shown in Figure 13, the BTL section imposes the maximum unscheduled down-time of about *138* hours to the PIP-II facility. This is mainly because of the fact that the BTL is the longest section of the facility with the length of around *350 m*. The second largest contributions of *120* hours come from the LB650 and SSR2 SRF sections. The SRF sections enforces a collective down-time of over *400* hours. However, this time shrinks to 65 hours in the fail-tolerance operating mode. The second largest contribution of 106 hours comes from the ion source in this mode of operation.

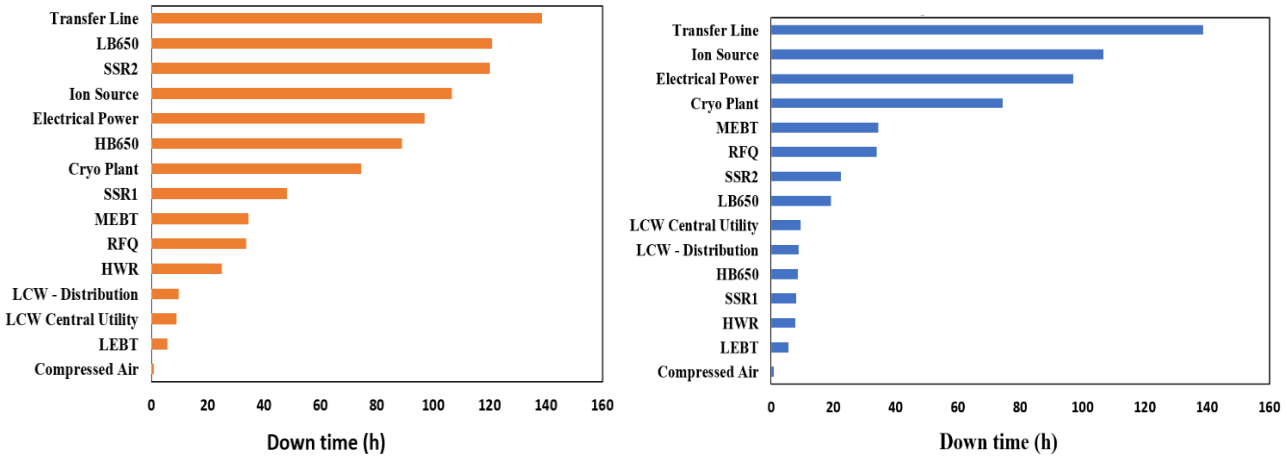

Figure 13: Distribution of the down-time hours by sections of the PIP-II facility operating in (left) no-failure-permit and (right) fail-tolerance modes. Note that, fail-tolerance of a cavity per section was applied only to the SRF sections of the facility.

E. Availability Assessment of PIP-II facility for Critical Operational Mode

In the critical operational mode, the PIP-II facility operates to deliver the beam at 600 MeV to the Booster Synchrotron. The difference of 200 MeV from the nominal energy is modelled by turning off additional SRF cavities in the linac. These cavities are treated as the spare cavities. Since the energy gain per cavity varies substantially along the linac (Figure 2), there are several combinations to obtain the total number of the spare cavities needed to downscale the beam energy from 800 MeV to 600 MeV. These combinations define states of the critical operational mode.

It is well known that most of the beam dynamics issues in an ion linac are associated with its low energy portion. To incorporate this fact in the availability analysis, it was assumed that there were no additional spare cavities in the HWR, SSR1 and SSR2 sections. For further simplification, it was considered that all the spare cavities were located only in one section. Thus, the critical operational mode was modelled for two cases representing all the spare cavities were located either in the LB650 or HB650 sections. Table 7 lists the number of the spare cavities in the respective sections. Note that,

transit time effect [37] has been included while evaluating the total number of the spared cavities in the respective sections. Table 7 lists the availability of the PIP-II facility for two cases of the critical operational mode. It can be discerned that the facility possesses about the same availability of 93 % in both cases as in the fail-tolerance nominal operational mode even after applying additional fail-tolerances in terms of the spare cavities. It is attributed to the fact that the quadrupole magnet package (as shown in Table 5) is the least available unit in both LB650 and HB650 sections that determines overall availability of these sections. Consequently, additional fail-tolerances of the SRF cavities bring in only a little impact on the availabilities of these sections and therefore, on the availability of the complete facility which is primarily governed by the least available BTL and ion source sections.

Table 7: Availability of the PIP-II facility for two cases of the critical operational mode.

Section	Total number of cavities	Spare cavities	A(%)
LB650	36	11	93.35
HB650	24	15	93.34

VI. SENSITIVITY ANALYSIS AND BENCHMARKING OF THE MODEL

A. Input Data Sensitivity Analysis

The quality of input data is the most crucial aspect of the availability analysis that needs to be assured to obtain a meaningful outcome from the analysis. On the contrary, because of the first-of-a-kind nature of every new accelerator, there are uncertainties involved with MTTF and MTTR data of the components. In order to attain an adequate level of confidence in outcome of the availability analysis, a sensitivity analysis was performed to understand the impact of a spread in the input data on the PIP-II availability.

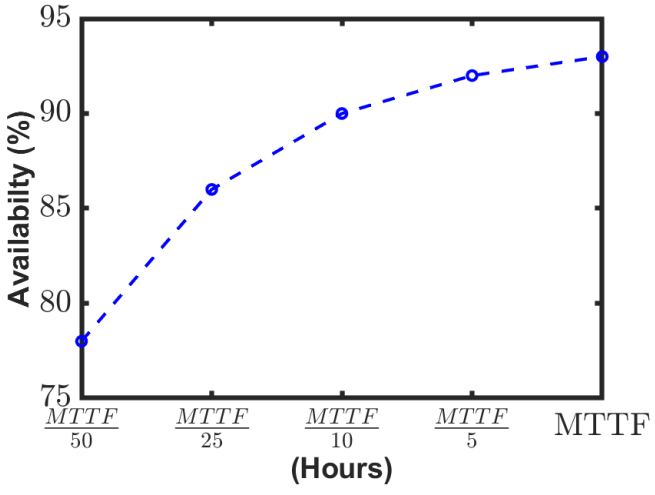

Figure 14: Variation in availability of the total facility with the MTTF scaling factor in a fail-tolerance operational mode.

It is evident that MTTF of a component is usually several order higher than its MTTR. In some cases (such as for the cavities), MTTF of a component could be higher from its life span. Consequently, MTTF data may possess a relatively higher uncertainty in comparison of the MTTR data especially for the large values due to a lack of the failure-rate statistics for such components. In order to analyse implication of uncertainty with the MTTF data in the PIP model, all components having MTTF above hundred years (*~10^6 hours)* were reduced by a scaling factor and then the facility availability was evaluated. Figure 14 shows the availability of the PIP-II facility in the fail-tolerance mode as a function of the MTTF scaling factor. It is apparent from here that the facility reaches to its target availability even after reducing the MTTF by a factor of ten. However, the availability degraded below *80%* after MTTF were scaled down by a factor of *50.* It can easily be concluded from Figure 15 that the SRF linac system availability is more sensitive to the fluctuations in MTTF data in comparison to the Utility and NC linac systems. Still, it attains the availability above *90%* even after applying the scaling factor of twenty-five to the MTTF data.

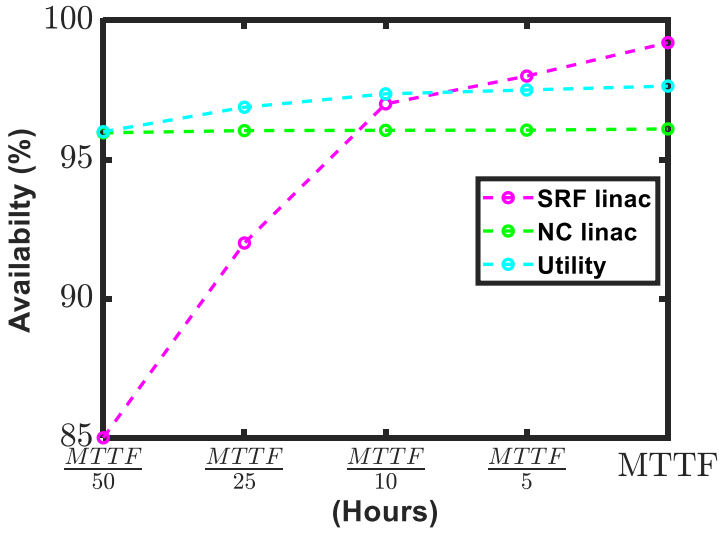

Figure 15: Availability of each major system in the PIP-II model as a function of MTTF scaling factor in a fail-tolerance operational mode.

In another approach to compute the least plausible availability of the PIP-II facility, it was assumed that the operational lifetime of the machine was thirty years. Accordingly, all the MTTFs beyond thirty years were reduced to 2.6×10^5 hours (equivalent to thirty years) in the model. In this scenario, the facility availability was found to be *71%.* Availabilities of the utility and NC linac systems were found to be *88%* and *95%* respectively while the SRF linac system obtained the availability of *85%.*

It can be concluded from the sensitivity analysis that the PIP-II model could even tolerate a spread of *96%* to the MTTF data above *~10^6 hours* without substantial impact on its target availability of *90%.* Also, among all three major systems,

the SRF linac system availability is affected most from the choice of the MTTF input data. However, even in a conservative estimate, the model predicted the PIP-II facility would have an up-time of *70%* of its total operational time with the SRF linac availability in high eighties.

A. Model Benchmarking

In order to validate the methodology developed for the PIP-II availability model, a reference model of the operational SRF linac of SNS accelerator facility at Oak Ridge was developed using the same methodology. The SNS SRF linac is an ideal choice for the reference model due to a close resemblance of its configuration and operational parameters to the PIP-II, LB650 and HB650 sections. The SRF linac design information was obtained from Ref. [33-35]. It has been designed to accelerate the beam from *180 MeV* to *1 GeV* using two families of SRF cavities. Accordingly, the SRF linac has been segmented in two sections: Medium Beta (MB) and High Beta (HB) sections. The MB section includes eleven cryomodules where each cryomodule houses three medium beta SRF cavities. The HB section consists of twelve cryomodules and, each cryomodule is composed of four high beta SRF cavities. There are normal conducting quadrupole doublets positioned between adjacent cryomodules to provide transverse beam focusing. The SRF cavities are powered individually using klystrons. Input data (MTTF and MTTR) for klystrons and associated RF components were obtained from Ref. [10] while the PIP-II input data were applied wherever they were applicable. Then, based on their functions, components in an SRF cryomodule of the SNS linac were grouped in the element packages. Appendix A3 provides a detailed composition and individual availabilities of each element package. Table 8 lists number of respective packages in MB and HB sections.

Table 8: Number of packages in MB and HB sections of the SNS SRF linac.

	MB	HB
Cavity Package	33	48
Magnet Package	22	24
Steerer Package	22	24
Cryo-Package	11	12
Transmitter	4	8
Modulator	3	4

The functional block diagram of the SRF linac system was prepared considering the element packages were connected to each other in a series configuration. The full SRF linac availability was then computed for the no-failure-permit and fail-tolerance operating modes. Note that, the fail-tolerance operating mode assumes one spare cavity in each section that might fail without interrupting the SRF linac operation. It can be observed from Table 9 that the model predicted the SRF linac system availability of *93%* and *99 %* in the respective no-failure-permit and fail-tolerance operating modes.

562 Table 9 : Operational availability of the SRF linac system of the SNS accelerator facility in two operational modes
563

	No-Failure-Permit Mode Availability	Fail-Tolerance-Mode Availability
	(%)	(%)
MB Section	97.2	99.4
HB Section	96.1	99.3
SRF linac	93.4	98.8

564

565 The operational statistics of the SNS SRF linac has been presented in Ref. [34-35] which shows availability of the
566 linac has been about *98%* since the fiscal year of 2011. It indicates the measured availability is in agreement with the
567 model predicted availability especially for the fail-tolerance mode where both matches within a percentage level. An
568 increase of five points with respect to the availability in the no-failure-permit mode may attribute to a conservative set of
569 the reliability input data. However, it has been addressed elsewhere [35] that the design energy of 1 GeV has yet to be
570 achieved for a nominal beam operation at the SNS accelerator facility. This is mainly because of collective effects (field-
571 emission, multi-pacting, heating etc.) limiting the operating accelerating gradient in the SRF cavities. In this case, one
572 can conclude that the fail-tolerance operating mode is a more representative choice to describe the SNS, SRF linac oper-
573 ation and therefore, the model predicted availability in this mode is in good agreement with the measured availability of
574 the SNS linac.

575 The PIP-II linac baseline incorporates SNS SRF linac operational experience in its design. The PIP-II SRF cavities
576 excludes usage of Higher Order Modes (HOMs) damper identified as roots of several associated problems (field emission,
577 heating, etc.) limiting RF performance of the accelerating cavities in SNS linac. A detailed study presented elsewhere [38]
578 concludes usage of HOMs dampers in SRF cavities are futile for the PIP-II SRF linac involving operation with a low
579 average beam current of 2 mA. In addition, uncorrelated HOMs spectrums of five families of the PIP-II SRF cavities,
580 HOMs frequency spread due to manufacturing errors and a lower HOMs impedances because of non-relativistic nature
581 of the beam, largely preclude most of the beam instabilities induced by HOMs. Thus, elimination of HOMs damper in
582 PIP-II SRF cavities is a preferable choice that lowers not only overall capital cost but also allows avoiding a number of
583 issues in SRF cavities. This in turn, could improve RF performance of the SRF cavities and hence the complete PIP-II
584 facility .

585

VII. SUMMARY

The paper introduced a methodology to model the availability of the complete particle accelerator facility. A comprehensive reliability model of the proposed PIP-II accelerator facility was developed that included not only the accelerator systems but also essential supporting systems such as the central cryo-plant, electrical power systems etc. The availability assessment of the PIP-II facility reveals that the ion source is most vulnerable system with availability of only 88%. Consequently, the baseline of the PIP-II facility adopted an additional ion source configured in the standby mode. This arrangement increases the ion source availability to 98.7%. The baseline design of the PIP-II SRF linac also attributes a cavity fault-tolerance in every SRF sections that enables the facility to operate in the fail-tolerance mode. Furthermore, the PIP-II integration and operation strategy plans for a fully functional spare cryomodule always available for each SRF section in inventory to minimize a repair time of the superconducting elements and therefore, unscheduled down time of the facility.

The availability of the full PIP-II facility in nominal operational mode was found to be 89 % that increased to 93% after introducing the fail-tolerance of a cavity in every SRF sections in the model. This corroborates that the baseline design of the PIP-II accelerator facility is sufficiently robust to meet the target availability in both nominal operational modes. Moreover, availability of the PIP-II facility was computed for the critical operational mode featuring the facility operation at the minimum beam energy of 600 MeV. The availability of the PIP-II facility in this mode was obtained to be 93%. An input data sensitivity analysis and the model validation using a reference model of the SNS SRF linac generate an adequate level of confidence in the PIP-II availability assessment that leads us further to initiate engineering design of the PIP-II facility.

ACKNOWLEDGEMENTS

The authors are thankful to the large team of scientists, engineers and technical staffs who provided key input data for this study. The authors would like to express gratitude on a more personal level to A. Klebaner, A. Martinez, J. Holzbauer, D. L. Newhart and, J. E. Anderson Jr. for their constructive suggestions and discussions that helped the authors to enhance quality of the paper. The author also wishes to acknowledge efforts of L. Serio and C. Adolphsen who reviewed this work and provided their invaluable feedback. The authors are also grateful to Barbara Merrill and Priyanka Saini for their invaluable time to proof-read the manuscript.

This manuscript has been authored by Fermi Research Alliance, LLC under Contract No. DE-AC02-07CH11359 with the U.S. Department of Energy, Office of Science, Office of High Energy Physics.

APPENDIX-A1

For the comprehension of this article, this appendix lists standard Reliability Engineering textbook formulae. Several of those formulae were applied in this article.

For of i^{th} component, if r_i = Reliability at any time *t*, a_i = Availability, λ_i = failure rate and μ_i = repair rate, then we can obtain following formulae.

1. *Series Configuration of the components in a system:*
    a. Availability of the system $A = \prod a_i$.
    b. Reliability $R = \prod r_i$.
    c. MTBF = $\frac{1}{\sum_i \lambda_i}$,
    d. Mean Time to Failure = $(1 - A) * MTBF$.
2. *Parallel Configuration of the components in a system*
    a. $1 - A = \prod (1 - a_i)$.
    b. $1 - R = \prod (1 - r_i)$.
    c. MTBF = $\frac{1}{(1-A)\sum_i \mu_i}$.
    d. Mean Time To failure = $(1 - A) * MTBF$
3. *k out of n systems:* Assume that all the components have same failure rate (λ) and repair rate (μ).
    a. $A = \sum_{i=0}^{k} \binom{n}{i} a^i (1-a)^{n-i}$ where, k is maximum number of failure allowed in a system, n is total number of components.
    b. MTBF = $\frac{1}{\lambda}\left(\frac{1}{n} + \frac{1}{n-1} + \cdots + \frac{1}{k}\right)$ for non-repairable systems.
4. *Standby (Cold):* A standby component implies that the component starts operating as soon as another component gets failed. Two components in a system have same failure rate (λ) and repair rate (μ) and one of the components is kept as standby mode, then reliability and MTBF of the system is expressed as below
    a. Reliability $R = (1 + \lambda t)e^{-\lambda t}$

b. $\text{MTBF} = \frac{2}{\lambda} + \frac{2\mu^2}{\lambda^2(\lambda+2\mu)}$

In general, when two components have different failure rate λ_1 & λ_2 and repair rate is μ_1 and μ_2, MTBF is then express as below

$$\text{MTBF} = \frac{1}{\lambda_1} + \frac{1}{\lambda_2} + \frac{\mu_1}{\lambda_2}\left(\frac{1}{\lambda_2} - \frac{1}{\lambda_2+\mu_1+\frac{\lambda_2}{\lambda_1}\mu_2}\right).$$

APPENDIX-A2

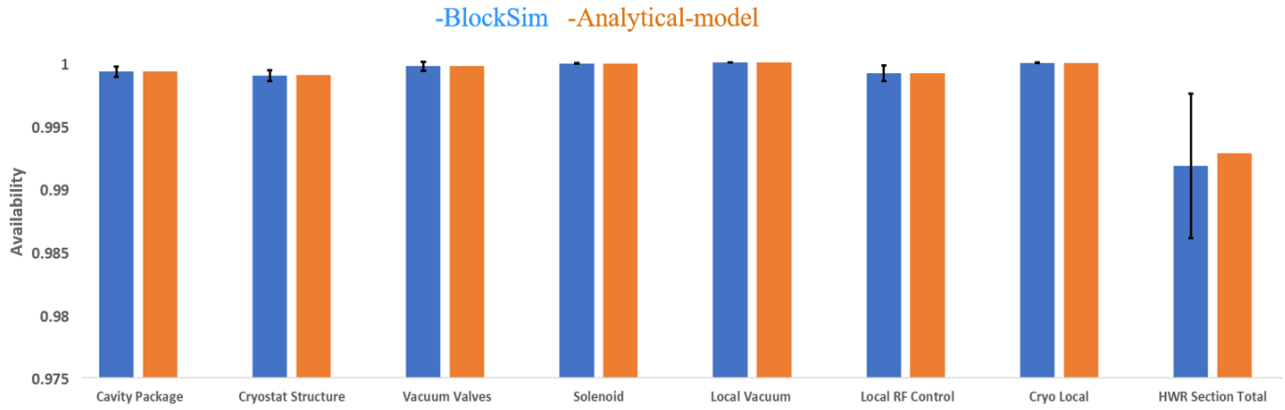

Figure A2: Availability of HWR cryomodule computed for no-failure-permit mode using BlockSim (blue coloured bars) and analytical model (saffron coloured bars).

APPENDIX-A3

A detailed view of the element packages in the SRF cryomodule of the SNS linac.

Packages	Components	MTTF	MTTR	A(%)
Magnet Package	Magnet	1E+06	16	
	Power Supply	4.6E+04	2	
	Magnet Instrumentation	1E+05	2	
Magnet Package Availability				99.99
Cavity Package	SRF Cavity	8.7E+08	776	
	Tuner	1E+06	216	
	Coupler	1E+07	0.5	
	Interlock Sensor	1E+05	1	
	Klystron	5E+04	4.5	
	Wave Guide	1.5E+05	3	
	Circulator	5E+04	3	
	Load	7.5E+04	3	
	LLRF	1E+05	2	
Cavity Package Availability				99.93
Steering Magnet Package	Steerer			
	Power Supply	1E+06	2	
	Magnet Instrumentation	1E+06	2	
	Steerer Instrumentation	1E+05	2	

Steering Magnet Package Availability				99.99
Cryo Package	Vacuum Valves	1E+07	8	
	Ion Pump	1E+06	4	
	Ion Pump Power Supply	1E+05	1	
	Local Cryogenic Distribution	5E+05	2	
Cryo-package availability				99.99
Additional Components	Transmitter	2.26E+04	4	99.98
	Modulator	5.6E+03	3	99.94

649

650

651 # REFERENCES

652 [1] J. N. Galayda, "The LCLS-II: A High-Power Upgrade to the LCLS," in proceedings of IPAC2018, Vancouver, Canada,
653 MOYGB2, pp. 18-23.

654 [2] S. Peggs et al, ESS Technical Design Report, 2013. http://inspirehep.net/record/1704813?ln=en

655 [3] A. Sharma, A. R. Jana, C. B. Patidar, M. K. Pal, N. Kulkarni, P. K. Hoyal, et al., Reference Physics Design for 1 GeV Injector
656 Linac and Accumulator Ring for Indian Spallation Neutron Source, arXiv:1609.04518 [physics.acc-ph]

657 [4] Zhihui Li, Peng Cheng, Huiping Geng, Zhen Guo, Yuan He, Cai Meng, Huafu Ouyang, Shilun Pei, Biao Sun, Jilei Sun, Jingyu
658 Tang, Fang Yan, Yao Yang, Chuang Zhang, and Zheng Yang, Phys. Rev. ST Accel. Beams 16, 080101 (2013)

659 [5] T. Himel, J. Nelson, N. Phinney, Availability and Reliability Issues for ILC, in proceedings of PAC07, Albuquerque, New Mex-
660 ico, USA (2007), pp. 1966–69.

661 [6] L. Burgazzi, P. Pierini , Reliability studies of a high-power proton accelerator for accelerator-driven system applications for nuclear
662 waste transmutation. Reliability Engineering and System Safety 2007; 92:449–63. https://doi.org/10.1016/j.ress.2005.12.008

663 [7] E. Bargalló, R. Andersson, A. Nordt, A. De Isusi, E. Pitcher, K. H. Andersen, ESS Availability and Reliability Approach, in pro-
664 ceedings of IPAC2015, Richmond, VA, USA (2015), MOPTY045, pp. 1033-35

665 [8] J. Knaster, P. Garin, H. Matsumoto, Y. Okumura, M. Sugimoto, F. Arbeiter, P. Cara, S. Chel, A. Facco, P. Favuzza, T. Furukawa,
666 R. Heidinger, A. Ibarra, T. Kanemura, A. Kasugai, H. Kondo, V. Massaut, J. Molla, G. Micciche, S. O'hira, K. Sakamoto, T. Yokomine
667 and E. Wakai, Overview of the IFMIF/EVEDA project, Nuclear Fusion, vol. 57, no. 10, pp. 102016, Jun, 2017,
668 https://doi.org/10.1088%2F1741-4326%2Faa6a6a

669 [9] R. Andersson, A. Nordt, E. Bargalló, Machine Protection Systems and Their Impact on Beam Availability and Accelerator Relia-
670 bility, in proceedings of IPAC2015, Richmond, VA, USA (2015), MOPTY044, pp. 1029-32

671 [10] P. Tallerico, D. Rees, D. Anderson, An Availability Model for the SNS Linac RF System, in proceedings of PAC2001, Chi-
672 cago, IL, USA(2001), MPPH112, pp. 1035-37.

673 [11] E. S. Lessner and P. N. Ostroumov, Reliability and availability in the RIA driver linac, in proceedings of PAC2005, Knoxville,
674 TN, USA (2005), FOAC005, pp. 443-445

[12] G. W. Dodson, Accelerator Systems RAM analysis, Talk in Accelerator Reliability Workshop, 2002, http://www.esrf.eu/files/live/sites/www/files/events/conferences/2002/ARW/proceedings/MONPM/Dodson.pdf

[13] M. J. Haire, Computation of Normal Conducting and Superconducting Linear Accelerator (Linac) Availabilities, ORNL, USA, Tech. Report, ORNL/TM-2000/93, 2000, https://www.osti.gov/biblio/885853-yUWMiH/

[14] PIP-II Conceptual Design Report, 2017, http://pip2-docdb.fnal.gov/cgi-bin/ShowDocument?docid=113

[15] E. L. Hubbard, Booster Synchrotron Report, 1973, https://lss.fnal.gov/archive/tm/TM-0405.pdf

[16] L. Merminga, PIP-II Global Requirements Document, FNAL, USA, PIP-II Document 1166-v8, ED0001222, 2020, https://pip2-docdb.fnal.gov/cgi-bin/RetrieveFile?docid=1166&filename=ED0001222%20PIP-II%20Global%20Requirements%20Document%20GRD.pdf&version=8

[17] A. Shemyakin, M. Alvarez, R. Andrews, J.-P. Carneiro, A. Chen, R. D'Arcy, B. Hanna, L. Prost, V. Scarpine, C. Wiesner, PIP-II Injector Test's Low Energy Beam Transport: Commissioning and Selected Measurements, AIP Conf. Proc., 1869, 050003 (2017).

[18] S. Virostek, *et al.*, Final Design of a CW Radio Frequency Quadrupole (RFQ) for the Project X Injector Experiment (PXIE), in *Proc. NAPAC'13*, Pasadena, CA, USA (2013), WEPMA21, pp. 1025-1027

[19] A. Saini, C. M. Baffes, A. Z. Chen, V. A. Lebedev, L. Prost, and A. Shemyakin, Design of PIP-II Medium Energy Beam Transport Beam, Proc. of IPAC 2018, Vancouver, Canada, 2018, TUPAF076, pp. 905-908.

[20] Z A Conway et al 2015 IOP Conf. Ser.: Mater. Sci. Eng.101 012019

[21] M. H. Awida *et al*., Development of Low □□Single-Spoke Resonators for the Front End of the Proton Improvement Plan-II at Fermilab, in *IEEE Transactions on Nuclear Science*, vol. 64, no. 9, pp. 2450-2464, Sept. 2017.

[22] V. Roger et al., Design Update of the SSR1 Cryomodule for PIP-II Project, in proceedings of IPAC2018, Vancouver, Canada (2018) WEPML019, pp. 2721-2723.

[23] A. Rowe, SRF Technology for PIP-II and PIP-III, in proc. SRF2017, Lanzhau, China (2017)

[24] A. Saini, "Design Considerations for the Fermilab PIP-II 800 MeV Superconducting Linac", Proc. of NA-PAC 2016, Chicago, USA, 2016, WEPOA60.

[25] Smith DJ. , Reliability, Maintainability and Risk, Elsevier Ltd; 2011. https://doi.org/10.1016/C2010-0-66333-4.

[26] Rausand M, Hsyland A. System Reliability Theory Models, Statistical Methods, and Applications SECOND EDITION. 2nd ed. JOHN WILEY & SONS, INC.

[27] Upadhyay J, Im D, Peshl J, Bašović M, Popović S, Valente-Feliciano AM, et al., Apparatus and method for plasma processing of SRF cavities. Nuclear Instruments and Methods in Physics Research, Section A: Accelerators, Spectrometers, Detectors and Associated Equipment 2016;818:76–81. https://doi.org/10.1016/j.nima.2016.02.049.

[28] A. Saini, J. –F. Ostiguy, N. Solyak and V. P. Yakovlev, Studies of Fault Scenarios in SC CW Project-X linac, in proceedings of NA-PAC2013**,** Pasadena, California, USA, 2013, MOPMA10, pp. 318-20

[29] Saini A, Solyak N, Yakovlev VP, Mishra S, Ranjan K. Study of effects of failure of beamline elements and its compensation in CW superconducting linac, in proceedings of IPAC2012, New Orleans, Louisiana, USA: 2012, p. 1173–75.

[30] P. F. Derwent, J.-P. Carniero, J. Edelen, V. Lebedev, L. Prost, A. Saini, A. Shemyakin, J. Steimel, PIP-II Injector Test: challenges and status, Proc. of LINAC'16, East Lansing, MI, USA, September 25-30, 2016, WE1A01

[31] A. Vivoli, J. Hunt, D. E. Johnson and V. Lebedev, Transfer Line Design for PIP-II Project, in proceedings of IPAC2015, Richmond, VA, USA (2015), THPF119, pp. 3989-3991

[32] https://www.reliasoft.com/products/blocksim-system-reliability-availability-maintainability-ram-analysis-software

[33] S. Henderson et al., The Spallation Neutron Source Beam Commissioning and Initial Operations, ORNL, USA, Tech. Report, ORNL/TM-2015/321, 2015, https://info.ornl.gov/sites/publications/files/Pub56465.pdf

[34] S.-H. Kim, R. Afanador, W. Blokland, M. Champion, A. Coleman, M. Crofford, et al., The status of the superconducting linac and SRF activities at the SNS, in: Proceedings of the 16th International Conference on RF superconductivity, Paris, France, September 23–27, 2013, pp. 83–88, http://accelconf.web.cern.ch/AccelConf/SRF2013/papers/mop007.PDF

[35] S. H. Kim et al., "Overview of ten-year operation of the superconducting linear accelerator at the Spallation Neutron Source," Nuclear Instruments and Methods in Physics Research Section A: Accelerators, Spectrometers, Detectors and Associated Equipment, Volume 852, 2017, Pages 20-32, ISSN 0168-9002, https://doi.org/10.1016/j.nima.2017.02.009.

[36] M. Convery et al., The PIP-II Preliminary Design Report, PIP-II Document 2261-v33, 2020, https://pip2-docdb.fnal.gov/cgi-bin/ShowDocument?docid=2261

[37] T. P. Wangler, RF Linear Accelerator, 2nd Edition, 2008, Wiley-VCH Verlag GmbH & Co.

[38] A. Sukhanov, A. Lunin, V. Yakovlev, M. Awida, M. Champion, C. Ginsburg, I. Gonin, C. Grimm, T. Khabiboulline, T. Nicol, Yu. Orlov, A. Saini, D. Sergatskiv, N. Solyak and A. Vostrikov, "Higher Order Modes in Project-X Linac,", Nuclear Instruments and Methods in Physics Research Section A, vol. 734, part A, pp. 9–22, 2014, https://doi.org/10.1016/j.nima.2013.06.113